Carbohydrate Polymers 339 (2024) 122268

Contents lists available at ScienceDirect

Carbohydrate Polymers

journal homepage: www.elsevier.com/locate/carbpol

The study of galactomannans with different molecular weights and their ability to form microparticles suitable for pulmonary delivery

Miguel F. Galrinho [a], Lisete M. Silva [a,*], Guido R. Lopes [a], Bernardo A.C. Ferreira [a], Sara A. Valente [a], Isabel Ferreira [b,c], Benedita A. Pinheiro [d,e], Angelina S. Palma [d,e], Dmitry V. Evtuguin [f], José A. Lopes da Silva [a], Margarida Almeida [g], Paula Ferreira [g], Maria T. Cruz [b,c], Manuel A. Coimbra [a], Cláudia P. Passos [a,*]

[a] LAQV-REQUIMTE, Department of Chemistry, University of Aveiro, 3810-193 Aveiro, Portugal
[b] Centro de Neurociências e Biologia Celular e Centro de Inovação em Biomedicina e Biotecnologia, Universidade de Coimbra, Azinhaga de Santa Comba, 3004-517 Coimbra, Portugal
[c] Faculdade de Farmácia da Universidade de Coimbra, Universidade de Coimbra, Pólo das Ciências da Saúde, Azinhaga de Santa Comba, 3000-548 Coimbra, Portugal
[d] UCIBIO, Applied Molecular Biosciences Unit, Department of Chemistry/Department of Life Sciences, School of Science and Technology, NOVA University of Lisbon, 2829-516 Lisbon, Portugal
[e] Associate Laboratory i4HB, Institute for Health and Bioeconomy, School of Science and Technology, NOVA University Lisbon, 2819-516, Caparica, Portugal
[f] CICECO, Aveiro Institute of Materials, Department of Chemistry, University of Aveiro, 3810-193 Aveiro, Portugal
[g] CICECO, Aveiro Institute of Materials, Department of Materials and Ceramic Engineering, University of Aveiro, 3810-193 Aveiro, Portugal

ARTICLE INFO

Keywords:
Carob
Microwave-assisted treatment
Structural analysis
Carbohydrate microarrays
Insulin
Microparticles

ABSTRACT

The influence of locust bean gum (LBG) galactomannans (GMs) molecular weight (Mw) to assemble microparticulate systems was evaluated, and carriers for deep lung delivery were developed. A commercial batch of LBG with a mannose/galactose (M/G) ratio of 2.4 (batch 1) was used to study the influence of different microwave partial acid hydrolysis conditions on carbohydrate composition, glycosidic linkages, and aqueous solutions viscosity. The microwave treatment did not affect the composition, presenting 4-Man (36–42 %), 4,6-Man (27–35 %), and T-Gal (24–25 %) as the main glycosidic linkages. Depolymerization led to a viscosity reduction (≤0.005 Pa·s) with no major impact on polysaccharide debranching. The structural composition of the LBG galactomannans were further elucidated with sequence-specific proteins using carbohydrate microarray technologies. A second batch of LBG (M/G 3.3) was used to study the impact of GMs with different Mw on microparticle assembling, characteristics, and insulin release kinetics. The low-Mw GMs microparticles led to a faster release (20 min) than the higher-Mw (40 min) ones, impacting the release kinetics. All microparticles exhibited a safety profile to cells of the respiratory tract. However, only the higher-Mw GMs allowed the assembly of microparticles with sizes suitable for this type of administration.

1. Introduction

Galactomannans (GMs) are neutral polysaccharides composed of a β-1,4-D-mannose backbone with single α-D-galactose residues linked at the *O*-6 position (Mccleary, Clark, Dea, & Rees, 1985). The high molecular weight of GMs results in poor solubility in water, and highly viscous solutions, even at low concentrations. Locust bean gum (LBG), also known as carob gum, is a source of GMs that are extracted from the seeds of *Ceratonia siliqua* L., a leguminous evergreen shrub, that naturally grows in the Mediterranean region.

The GMs of LBG are reported to present a mannose/galactose (M/G) ratio of approximately 4:1, distinctive from GMs of other sources, such as tara, guar, and fenugreek gums, accounting for M/G ratios of 3:1, 2:1 and 1:1, respectively (Prajapati, Jani, Moradiya, Randeria, & Nagar, 2013; Srivastava & Kapoor, 2005). However, environmental factors and extraction methods may result in GMs with distinct M/G ratios and, consequently, different physicochemical features (Cerqueira et al., 2009; Chaires-Martínez, Salazar-Montoya, & Ramos-Ramírez, 2008; Passos, Moreira, Domingues, Evtuguin, & Coimbra, 2014; Simões, Nunes, Domingues, & Coimbra, 2010). The solubility of GMs in water is

* Corresponding authors.
E-mail addresses: lisete.silva@ua.pt (L.M. Silva), cpassos@ua.pt (C.P. Passos).

https://doi.org/10.1016/j.carbpol.2024.122268
Received 29 January 2024; Received in revised form 7 May 2024; Accepted 12 May 2024
Available online 22 May 2024

higher for polysaccharides with lower M/G ratios (Brito-Oliveira, Cavini, Ferreira, Moraes, & Pinho, 2020; Hellebois et al., 2021; McCleary, Amado, Waibel, & Neukom, 1981), due to the existence of a greater number of galactose single residues within the mannose chain, which keeps them from creating intermolecular interactions (Kontogiorgos, 2019).

Galactomannans biodegradability and low toxicity have shown potential for applications in pharmaceutical areas (Dionísio & Grenha, 2012). As a result, these polysaccharides have been explored in several alternative drug delivery systems (including oral, buccal, ocular, topical, and colon) as carriers (Dionísio & Grenha, 2012; Prajapati et al., 2013), allowing the protection of the encapsulated agent and its controlled release (Avachat, Dash, & Shrotriya, 2011; Gowda, Gupta, Khan, & Singh, 2011). Another non-invasive alternative system for drug delivery that has been gaining attention for drug administration is pulmonary delivery. Indeed, the alveoli's large surface area (>100 m^2) (Stone, Mercer, Gehr, Stockstill, & Crapo, 1992), thin epithelium (<1 μm thick) (Weibel, 1963; Weibel, 2017), high blood supply and permeability, are among the most prominent advantages associated to this route (Valente et al., 2022). Inhalable powders can offer many advantages for this type of administration such as easy storage and high stability (Cavaiola & Edelman, 2014). Among the different pharmaceuticals investigated, insulin has received significant attention. For insulin delivery, the assembly of inhalable particles using polysaccharides such as GMs as carriers (Valente et al., 2022; Valente et al., 2023) may ensure a local or systemic action of the pharmaceutical cargo. The pulmonary delivery system requires microparticles with an appropriate aerodynamic diameter (1–5 μm) to reach the alveolar zone, which can be achieved using spray-drying if the viscosity of the polymeric solution is below 0.3 Pa·s (Alves et al., 2016; Arpagaus & Meuri, 2010). This means that, for the use of GMs, only very diluted solutions could be used due to their high viscosity. GMs from LBG have shown their potential in pulmonary delivery as carriers of tuberculosis-treating drugs (Alves et al., 2016), thus representing an alternative delivery method to treat this disease (Rodrigues et al., 2017). Nevertheless, the preparation could only allow the use of 2 % (*w/v*) of GMs after a difficult solubilization procedure under acidic conditions, which may represent a bottleneck process for scale-up. Furthermore, to our knowledge, applications regarding GM-based carriers via this route are still scarce, possibly due to the technological difficulties of processing high-viscous solutions. For GMs with high M/G ratios, partial acid hydrolysis assisted by microwave can be advantageous, changing physicochemical properties and promoting depolymerization, decreasing GM viscosity (Passos et al., 2019).

In addition to the structural analysis by gas chromatography, this work explores the structural features of the studied galactomannans using carbohydrate microarray technologies. The galactomannans were structurally adapted to allow a feasible method for insulin administration, investigating the possibility of assembling a GM particulate system as a carrier. By atomizing different-sized fractions of GMs in the presence of insulin, it is aimed to obtain a variable shape and size distribution and to determine which would better fit the dimensions for more efficient pulmonary delivery.

2. Material and methods

2.1. Galactomannan sources and preparation

Galactomannans (GMs) from commercial locust bean gum (LBG) were purchased from Sigma-Aldrich (G0753 - Locust bean gum from *Ceratonia siliqua* seeds). Two batches were used: batch 1 (#126H0134) was used to study the influence on sugar composition, glycosidic linkages, and viscosity of aqueous solutions of GMs resultant from microwave partial acid hydrolysis conditions; batch 2 (#SLCD9879), was used to study the influence of the Mw of GMs fractions produced by microwave partial acid hydrolysis on particles morphology, size, and insulin release to an aqueous solution.

2.1.1. Microwave-assisted (MW) partial acid hydrolysis

To perform the partial acid hydrolysis of the LBG galactomannans, 3 g of LBG powder was dispersed in 3 mL of ethanol, followed by the addition of 60 mL of 0.3 M acetic acid under continuous stirring with a magnetic bar to prevent granulation. A microwave oven (MicroSYNTH Labstation, maximum output 1 kW, 2.45 GHz, Milestone Srl., Bergamo, Italy) was used with 4 high-pressure closed reactors of 100 mL capacity. The programs started at room temperature with a heating ramp of 25 °C/min, followed by 2 min of isocratic heating at settled temperatures of 130, 150, or 165 °C, based on previous works (Passos & Coimbra, 2013; Passos et al., 2014; Passos, Rudnitskaya, Neves, Lopes, Evtuguin, & Coimbra, 2019). Each solution was filtered, and an aliquot of the filtrate was frozen and freeze-dried for estimation of the solubilized mass. To correlate the interactions between the mass of LBG (**m**), reaction temperature (**T**), and acetic acid concentration (**Ac**), a two-level factorial design was performed (Supplementary Table S1 and Fig. S1).

2.1.2. Rheological (viscosity) and molecular weight assessment

Rheological tests were performed in steady-shear flow for LBG galactomannan solutions at 15 mg/mL. The isothermal measurements (20 °C) were performed on a TA AR-1000 rheometer (TA Instruments, Surrey, England) with a cone-and-plate device (acrylic, 6 cm diameter, angle 2°) (Cardoso, Coimbra, & Lopes da Silva, 2003). Flow curves were obtained by applying a stress ramp from 0.05 to 3 Pa. The apparent viscosity was taken at a shear rate of 60 s^{-1}.

The average molecular weight (Mw) of the samples was determined by size exclusion chromatography using 0.1 M $NaNO_3$ aqueous solution as eluent (Passos, Cepeda, et al., 2014). The analysis was performed using two PL aquagel−OH MIXED 8 μm columns (300 × 7.5 mm) protected by a PL aquagel-OH Guard 8 μm pre-column on a PL-Gel Permeation Chromatograph (GPC) 110 system (Polymer Laboratories, Shropshire, UK) equipped with refractive index (RI) detector at 36 °C. The columns were calibrated with pullulan standards (Polymer Laboratories, Shropshire, UK) in the range of 0.7–1600 kDa, and glucose was used as an internal standard. Data analysis was performed using CIRRUS™ GPC/Multidetector Software (Polymer Laboratories, Shropshire, UK).

2.1.3. Fractionation by ultrafiltration

The MW-treated samples were subjected to ultrafiltration using a Millipore Labscale TFF system as previously described in Passos et al. (2021). A set of membranes of different molecular weights (Pellicon XL with Biomax®) were used in the following sequence order: MWCO 300, 100, 50, 30, and 10 kDa, operating at room temperature and working at 10 to 20 psi transmembrane pressure, 20–40 psi and 10–20 psi, respectively in the "feed-in" and "retentate-out" sections of the equipment. All retentate and the final permeate (molecular weight < 10 kDa) were recovered, frozen, and freeze-dried.

2.2. Galactomannan analysis

2.2.1. Sugars and glycosidic linkage composition

Neutral sugars were assessed as alditol acetates following established protocols (Passos & Coimbra, 2013). In brief, 1–2 mg of each sample was weighed and solvated in 200 μL of 2 M H_2SO_4 and 1 mL of distillate water. The hydrolysis occurred at 120 °C for 60 min and 200 μL of 2-deoxy-glucose (1.0 mg/mL and 3.0 mg/mL for the free and neutral sugars, respectively) was added as an internal standard. From this solution, 500 μL was neutralized with 200 μL of 25 % NH_3. Alditol acetates were prepared by reduction with 100 μL of $NaBH_4$ (15 % (*w/v*) in 3 M NH_3) at 30 °C for 1 h. Excess $NaBH_4$ was destroyed with acetic acid. Acetylation occurred in 300 μL of the previous solution at 30 °C for 30 min with 3 mL of acetic anhydride, using 450 μL of 1-methyl imidazole as the catalyst. By adding 3 mL of water and 2.5 mL of dichloromethane and stirring, the alditol acetates were transferred from the water to the organic phase. The two phases were separated by centrifugation (3000

rpm, 30 s, room temperature). The water phase was removed, and the organic phase evaporated. The alditol acetates were solubilized in anhydrous acetone. The analysis was performed by gas chromatography (GC) with a flame ionization detector (FID) (Perkin-Elmer Clarus 400 gas chromatographer) equipped with a 30 m × 0.25 mm DB-225 capillary column (Agilent J&W GC columns, USA).

The glycosidic linkages of the galactomannan samples were determined by methylation analysis by dissolving 1–2 mg of samples and following the $NaOH/Me_2SO/CH_3I$ method (Ciucanu & Kerek, 1984). A re-methylation procedure was performed to ensure complete methylation of the polysaccharides. The re-methylated galactomannans were hydrolysed with 2 M TFA at 120 °C for 60 min; reduced with $NaBD_4$ (in 2 M NH_3) at 30 °C for 60 min and acetylated with acetic anhydride at 30 °C for 30 min in the presence of 1-methylimidazole (Coimbra, Delgadillo, Waldron, & Selvendran, 1996; Harris, Henry, Blakeney, & Stone, 1984). The partially methylated alditol acetates were analyzed by GC–MS (GC-qMS, Shimadzu GC–MS-QP2010) as described (Passos, Rudnitskaya, Neves, Lopes, & Coimbra, 2019).

2.2.2. Carbohydrate microarray construction and analysis

A total of nine LBG GM-derived fractions obtained after microwave treatment and/or ultrafiltration process were analyzed in a carbohydrate microarray format. Five commercial polysaccharides including galactomannans from LBG and guar, a glucomannan, and an arabinogalactan were included as controls for array validation and comparison purposes. The list of polysaccharides included in the microarray, their sources, and their main composition is given in Supplementary Table S2. Details on the carbohydrate samples, microarray construction, printing conditions, imaging, and data analysis are compliant with the Minimum Information Required for A Glycomics Experiment (MIRAGE) guidelines for reporting glycan microarray-based data (Liu et al., 2016; Palma et al., 2015).

The microarray was constructed as described by Reis et al. (2023) and was probed with six carbohydrate-binding proteins with reported specificities including three monoclonal antibodies against β1,4-mannan and galactomannan, two plant lectins, and one mammalian immune receptor. Information on their names, sources, conditions of analysis, and their reported carbohydrate specificity is detailed in Supplementary Table S3. The microarray binding analysis was performed essentially as previously described (Liu et al., 2012). For the biotinylated plant lectins *Ricinus communis* agglutinin-I (RCA_{120}) and Concanavalin A (ConA), nitrocellulose nonspecific binding sites were blocked for 60 min with 3 % (*w/v*) bovine serum albumin (BSA, Sigma) in 10 mM HEPES pH 7.3, 150 mM NaCl (referred to as HBS), supplemented with 5 mM $CaCl_2$, followed by the overlay, for 90 min, with the different proteins diluted in the blocking solutions to the final concentration of 5 mg/mL (Supplementary Table S3). For the monoclonal antibodies and the mammalian lectin, microarray slides were blocked with 1 % (w/v) BSA, 0.02 % (*v*/v) casein in HBS, 5 mM $CaCl_2$, the microarrays were overlaid for 90 min with the antibody solutions prepared to the final concentration concentrations/dilutions given in Supplementary Table S3, followed by incubation with the corresponding detection reagents in specified blocking solutions for 60 min. The detection reagents without the proteins were also analyzed to detect any nonspecific binding. For all the microarray analyses, the Alexa Fluor-647-labeled streptavidin (1 μg/mL, Molecular Probes, S21374), diluted in the corresponding blocking solutions, was added to each pad, incubated for 30 min, and used as fluorescence reagent for readout, using a GenePix® 4300A fluorescence scanner (Molecular Devices). Microarray data quantitation was done using the GenePix® Pro Software (Molecular Devices).

2.3. Galactomannan-based microparticles preparation and analysis

LBG galactomannan-based microparticles were prepared by solubilizing 180 mg of each fraction in 20 mL of distilled water. The pH was adjusted with HCl (2 M) to a range between 4 and 5. Aliquots of 20 mg of insulin were dissolved in 1 mL of HCl (0.01 M) and added to the solubilized fractions achieving a final mass concentration of approximately 10 mg/mL, containing 10 % of insulin (*w*/w). More detailed information on the procedures described in this section can be found in Valente et al. (2023).

2.3.1. Particles assembling by spray-drying

The particles were prepared by spray-drying using a BÜCHI Mini Spray Dryer B-191 (Büchi Labortechnik AG, Flawil, Switzerland) equipped with a high-efficiency cyclone. The conditions were as follows: an inlet temperature of 150 °C, outlet temperature of 60 °C, aspiration of 95 %, pump at 12 % (aspiration and pump percentages are related to the maximum allowed by the equipment), and a flux of 3.6 mL/min.

2.3.2. Particles characterization by scanning electron microscopy (SEM)

To study the morphology and the size distribution of the particles obtained, the atomized powders were placed in a support with a copper strip and analyzed by SEM as described in Valente et al. (2023). Briefly, samples were coated with a conductive material using a carbon evaporator sputter Emitech K950X and observed in an electron microscope Hitachi S4100 operating at 25 kV. Images were treated using the ImageJ software (Schneider, Rasband, & Eliceiri, 2012). Particle sizes were determined by quantifying the volume of at least 50 particles in the micrographs, with particle volume distributed according to Valente et al. (2023).

2.3.3. Cell culture and cytotoxicity assay

Cell toxicity assays were performed in the mouse leukemic monocyte macrophage cell line RAW 264.7 (ATCC Cat# TIB-71, RRID:CVCL_0493) and in the human lung adenocarcinoma alveolar epithelial cell line A549 (ATCC Cat# CCL-185, RRID: CVCL_0023) using the resazurin reduction assay, as previously described by Valente et al. (2023). Cellular assays were carried out in three independent experiments, each performed in duplicate.

One-way ANOVA with Dunnett's multiple comparisons test was performed to compare treated with untreated cells (Ctrl). The *p*-value <0.05 was accepted as denoting statistical significance. All analyses were conducted using GraphPad Prism version 8 for macOS (GraphPad Prism, RRID: SCR_002798).

2.3.4. Insulin release kinetics

Insulin release kinetics were evaluated following literature (Alves et al., 2016) and processed as detailed in Valente et al. (2023). A solution of 0.01 M phosphate-buffered saline (PBS, pH 7.4) and 1 % (*V*/V) of Tween80 was used to simulate the lung fluid. High-performance liquid chromatographer (HPLC) with Diode Array detector (model Ultimate 3000) was used with a C18 column LiChrospher® RP-18 (5 μm particle size, I.D. 25 cm × 4.6 mm, end-capped), using the chromatographic separation conditions of Amidi et al. (2008).

3. Results and discussion

3.1. Characterization of locust bean gum (LBG) galactomannans (GMs)

3.1.1. Carbohydrate composition

LBG galactomannans used in the present work were from two different commercial batches (Sigma-Aldrich) obtained from *Ceratonia siliqua* seeds. Batch 1 contained 80 % of carbohydrates, mainly composed of mannose (Man, 67 mol%) and galactose (Gal, 28 mol%), with a small content of glucose (Glc, 3 mol%) and arabinose (Ara, 2 mol %) residues (Table 1), consistent with a GMs composition. This batch showed a Man to Gal ratio (M/G) of 2.4, slightly lower than the M/G ratio reported in the literature for LBG GMs, which typically varies between 3 and 4 (Kök, 2007; Lazaridou, Biliaderis, & Izydorczyk, 2001). On the contrary, batch 2 had an M/G ratio of 3.3, within the reported range, with 85 % carbohydrates, where mannose accounted for 74 mol%

Table 1
Carbohydrate composition, total carbohydrate content, and mannose/galactose (M/G) ratio of the crude LBG samples studied.

	Total sugars (%)	Sugar composition (mol %)				M/G ratio
		Ara	Man	Gal	Glc	
Batch 1	80.2 ± 9.4	1.9 ± 0.1	67.4 ± 0.9	27.7 ± 1.0	2.9 ± 0.0	2.4
Batch 2	84.9 ± 1.1	1.2 ± 0.0	73.9 ± 0.3	22.4 ± 0.0	2.4 ± 0.3	3.3

Ara, arabinose; Man, mannose; Gal, galactose; Glc, glucose.

and galactose for 22 mol%. Aiming to further elucidate the structural composition of the different batches of LBG galactomannans, these were probed for recognition with sequence-specific proteins using carbohydrate microarray technologies.

3.1.2. Carbohydrate microarray construction and analysis with sequence-specific proteins

A focused carbohydrate microarray was constructed containing the nine LBG-rich samples (positions #1–#9, Supplementary Table S2). Commercial polysaccharides, such as galactomannans from other sources (LBG and Guar, including a Gal depleted mannan), a glucomannan, and an arabinoxylan were also included to increase the structural diversity of the array and for validation purposes (positions #10–#14, Supplementary Table S2). The microarray was probed for recognition with carbohydrate-binding proteins with known carbohydrate-binding specificity. These include the linear β-1,4-mannan-specific monoclonal antibodies (mAbs) 400–4 and LM21, and the anti-galactomannan mAb CCRC-M70; two plant lectins: concanavalin A (ConA) and *Ricinus communis* agglutinin-I (RCA120) and the mammalian lectin from the human innate immune system DC-SIGN (Supplementary Table S3). Distinct binding patterns of these proteins were observed in the samples included in the array, showing a good correlation with reported specificities of the polysaccharides, which served as validation and quality control of the analysis. The results of the microarray binding analysis are shown in Fig. 1. The β-1,4-linked mannose-specific monoclonal antibodies 400-4 and LM21 presented a similar microarray binding profile (Fig. 1a). However binding signals were overall stronger with the 400-4 (0-50 k glycan binding intensity) than with the LM21 (0–5k glycan binding intensity). As expected, binding was detected to LBG and guar galactomannans, as well as to the glucomannan included in the array as controls (Fig. 1a). Both antibodies recognized the LBG fractions from batches 1 and 2. A strong and restricted binding was detected with CCRC-M70 to the galactomannans from batch 1 and to the control guar, suggesting the requirement of this antibody for a lower M/G ratio of galactose substitution (Fig. 1a). These results are in agreement with a recent study that showed evidence for lower Man/Gal ratios in oligosaccharide sequences and recognition of a galactosylated epitope by CCRC-M70 (Ribeiro, 2020). Interestingly, low binding was observed to the LBG from batch 2, and negligible binding was detected to the GMs from the control LBG. These microarray data point to a structural

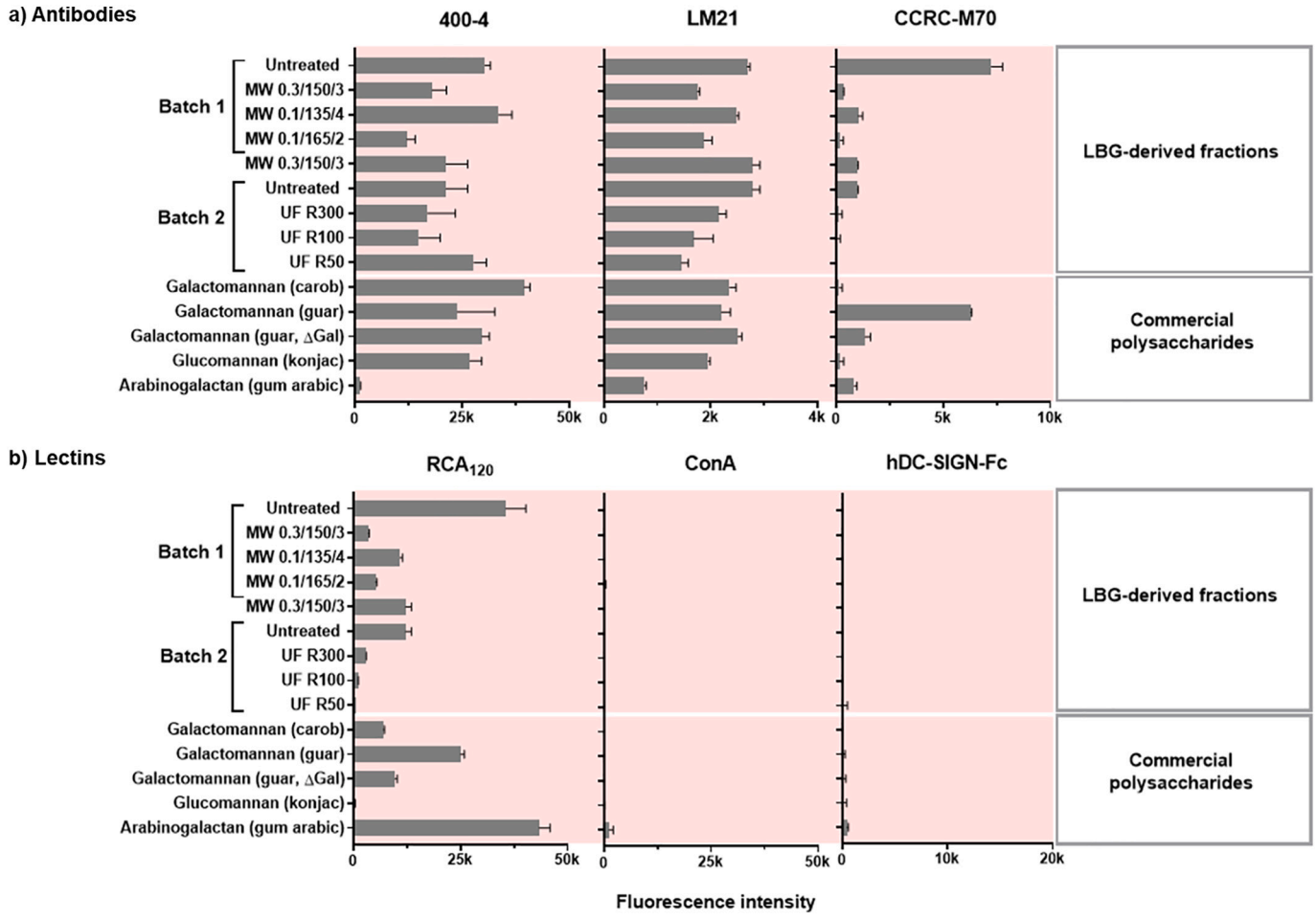

Fig. 1. Carbohydrate microarray analyses of the binding of a) monoclonal antibodies and b) lectins to galactomannan fractions and commercial LBG polysaccharides. Detailed information on the polysaccharides and proteins analyzed is in Supplementary Tables S2 and S3, respectively. The scales for the glycan binding intensities (fluorescence) are depicted at the bottom for each protein; these are means of fluorescence intensities of triplicate spots arrayed (with error bars) at 0.5 mg/mL per spot.

difference for the GMs between LBG from batch 1 and batch 2, suggesting that the GM of LBG from batch 1 has a chemical structure closer to that of guar galactomannan instead of GMs from LBG stated as control. The plant lectin RCA120, known to recognize non-reducing terminal β-Gal residues (Supplemented Table S3), bound to the arabinogalactan included as a control, a polysaccharide that contains non-reducing terminal β-Gal residues. Nevertheless, it was also observed that it bound strongly to the untreated LBG galactomannans from batch 1 and to guar galactomannan (Fig. 1b). These galactomannans do not contain non-reducing terminal β-Gal residues, but highly substituted α-1,6-Gal residues, showing that RCA120 may also recognize highly substituted galactomannans. As expected, no binding was detected to the LBG GMs studied (composed of β-1,4-linked mannan backbone with α-1,6-galactose branches) with concanavalin A (ConA), a plant lectin with specific recognition to α-Man residues (Fig. 1b). Similarly, no binding was observed to any of the LBG samples with the mammalian immune receptor hDC-SIGN (Fig. 1b), reported to have a broad carbohydrate specificity (Supplementary Table S3), pointing to the potential application of these galactomannans that do not involve immune recognition, such as the case when using these polysaccharides as carriers for drug delivery.

3.2. Galactomannan microwave treatment and fractionation

3.2.1. Microwave-assisted partial acid hydrolysis

Because LBG galactomannans form viscous solutions even at low concentrations, microwave-assisted (MW) partial acid hydrolysis was carried out, aiming at GM depolymerization and consequent decrease in viscosity, without complete degradation of the polysaccharide.

The optimization of the process conditions (performed on LBG samples from batch 1) was based on a two-level factorial design to correlate interactions between 3 factors: acid concentration, reaction temperature, and mass of LBG (Supplementary Table S1 and Fig. S1). The influence of the MW treatment on the molecular weight and viscosity of the samples was studied, and these are represented in Fig. 2a and b, respectively.

The flow curves obtained from the rheological tests showed the typical shear-thinning behaviour of random-coil polysaccharides at this concentration range (results not shown). The viscosity measured at 60 s^{-1} was considered to compare the apparent viscosity among samples. MW-partial acid hydrolysis of the LBG galactomannans resulted in an effective reduction of the molecular weight and viscosity of the samples (Fig. 2a and b). No significant downward trend was observed above 135 °C. The results shown in the Pareto chart (Fig. S2, Supplementary Material), showed temperature as the main contributor to this effect. In all experiments, the sample concentrations obtained after the MW treatment (~20 mg/mL) or the concentration when using the retentate extracts after re-dissolution (10 mg/mL) all fit the spray-drying requirement for viscosity (<0.3 Pa·s) (Fig. S3, supplementary material) (Alves et al., 2016; Arpagaus & Meuri, 2010).

The GM fractions resulting from the process conditions performed at 135 °C, led to samples with the highest viscosity (0.015–0.05 Pa·s, Fig. 2b). After drying, the sample treated under the condition 0.5/135/4 (acetic acid concentration (M), temperature (°C), mass (g)) (Supplementary Table S1), was redissolved, and the viscosity was seen to be proportional to concentration, being that the viscosity highly increased as the concentration was incremented (Supplementary Fig. S3).

Samples obtained after MW treatment at 135 °C presented viscosities of 0.015–0.035 Pa·s, which proved to be very difficult to ultrafiltrate, resulting in clogging effects if not very diluted. Furthermore, these GM fractions were not considered in proper conditions to continue the ultrafiltration molecular weight separation. For this reason, all the samples obtained under this temperature were not ultrafiltered and were further processed as they were recovered from the MW reactor. A similar reduction of the viscosity and molecular weight can be observed when using reaction temperatures of 150 °C and 165 °C, both resulting in low

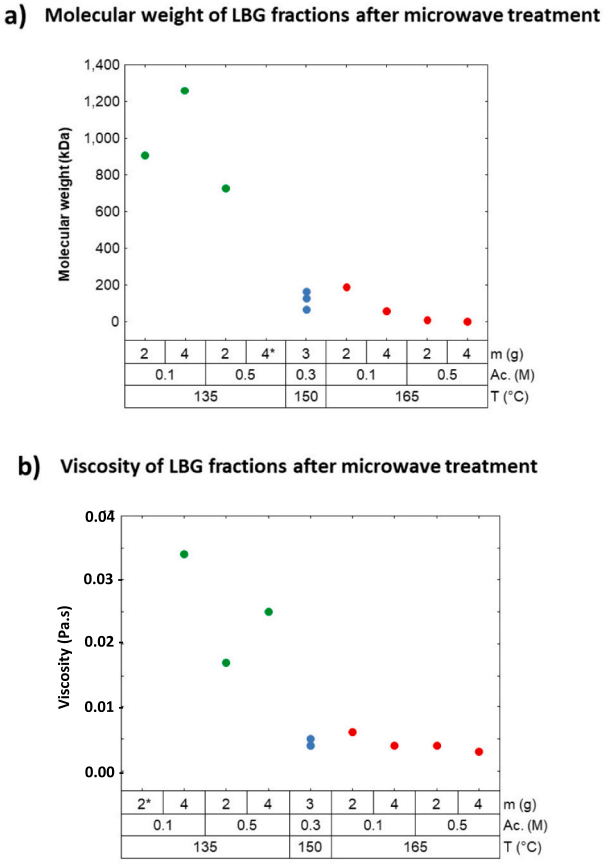

Fig. 2. The influence of factors: temperature (T, °C), acetic acid concentration (Ac, M), and mass content in the reactor (m, g) during microwave treatments. Impact on the molecular weight (a) and viscosity (b) of the LBG galactomannans. Data related to the conditions at $T = 135$ °C (green); $T = 150$ °C (blue), and $T = 165$ °C (red). *No data is available due to the high viscosity of the samples.

viscosity samples (<0.005 Pa·s, Fig. 2b). Because the 150 °C condition, also named as central point (0.3 M acetic acid, 150 °C, and 3 g LBG, 0.3/150/3), requires a lower energy consumption for the MW treatment when compared with those treated at 165 °C, this was the selected condition to carry out the large-scale analyses using batch 2.

3.2.2. Fractionation by ultrafiltration

A fractionation of MW-treated LBG (batch 2, central point condition) was performed using a series of ultrafiltration membranes to isolate galactomannans of different Mw. A sequential process using 5 membranes was used, starting with the 300 kDa cut-off membrane, followed by the membranes with a cut-off of 100 kDa, 50 kDa, 30 kDa, and 10 kDa. The correspondent retentates (>300 kDa, 100–300 kDa, 50–100 kDa, 30–50 kDa, 10–30 kDa, respectively) were recovered. An additional permeate fraction was obtained at the final step corresponding to a content <10 kDa. All fractions were freeze-dried to account for yield and further characterized and prepared for microparticles (Mp) assembly.

The first membrane, with a 300 kDa cut-off, was only able to separate 375 mL of permeate from the initial 500 mL. While increasing the sample concentration, the increasing pressure observed, did not allow the ultrafiltration to proceed further. Whenever the ultrafiltration working conditions were exceeded (among 10 and 20 psi transmembrane pressures) the process had to be stopped and the solution diluted to continue the ultrafiltration process and avoid clogging effects. The increase in pressure during the ultrafiltration process was less

evident for the remaining fractions. This effect shows the impact of the presence of high molecular weight GMs in the >300 kDa retentate which highly increases viscosity when concentrated. A brown colour appeared after the MW treatment. As the fractions were separated, the retentates became white to light yellow, and it was on the final permeate fraction that the darker yellow to orange colour remained. The colour can also be an effect of depolymerization and formation of low molecular weight compounds, such as free sugars, but also from the formation of new ones by caramelization and/or Maillard reactions occurring during the MW-heat treatment (Morales & van Boekel, 1998).

The yield obtained as retentate in each step of the ultrafiltration, about the corresponding microwave-treated sample (UF η, %) is presented in Table 2, with a total mass of 5.5 g. This recovery corresponds to 60 % of the mass that was initially recovered after the MW treatment (joining the soluble fraction from 4 reactors). Therefore, about 40 % of the mass used in the UF filtration processing was lost, mainly by fouling into the UF membranes. This phenomenon has been described for UF processes when polysaccharides are present (Lee, Amy, Croué, & Buisson, 2004), and is exacerbated when using high-concentration and/or very viscous samples. Additionally, adsorption of lower molecular weight compounds to the polymeric membrane may also be occurring, an effect that has been observed and is more evidenced in the presence of free sugars (Passos et al., 2021). To reduce the adsorption effects, each sample was ultrafiltered twice. Analyzing the yield for the fractions recovered with UF (Table 2), it was possible to conclude that the MW treatment led mainly to the formation of polymers with molecular weight superior to 300 kDa (17 %) and inferior to 10 kDa (30 %, data not shown). Yields for the retentates obtained by UF with cut-offs of 100, 50, and 30 kDa were all <5 % each (Table 2). The material recovered between 30 and 50 kDa resulted in the lowest quantity of mass and was not used for the development of Mp (Section 3.3.1).

3.2.3. *Structural analysis of galactomannan fractions upon MW treatment*

The glycosidic linkage analysis of batch 1 allowed to identify 4-Man (36 %), 4,6-Man (35 %), and terminally-linked Gal (T-Gal, 25 %) as the main sugar residues (Table 2), characteristic linkages of LBG galactomannans (Simões, Nunes, Domingues, & Coimbra, 2011). Considering the M/G ratio of 2.8 determined from glycosidic linkage results (Table 2), it showed some differences when compared with 2.4, the value obtained by sugar analysis (Table 1). Regarding batch 2, it was identified the same predominant linkages, with 4-Man (48 %), 4,6-Man (17 %), and T-Gal (15 %). Batch 2 showed a similar tendency to batch 1, with differences when comparing results from methylation (4.8) and neutral sugar analysis (3.3). These differences can be the result of some heterogeneity in the powder, especially in the case of GMs with a lower DB, which may not have been completely solubilized before the MW treatment. Nevertheless, a relatively high mol % of 4,6-Man residues in the galactomannans was observed (Table 2) and could not be correlated with the correspondent T-Gal units present as side chains (single branching residues). In all samples, it was possible to identify the presence of 8–12 % of mannose ramifications that were not substituted with a Gal residue. For the missing Gal that could not be accounted for, two possible hypotheses could explain such differences: firstly, it could be a consequence of the degradation of free Gal residues after debranching from the microwave treatment, where the acidic conditions and temperature could destroy these monosaccharides. The other hypothesis is related to the use of acetic acid during the microwave process, which can lead to a chemical acetylation of the main chain, as demonstrated in the literature (de Oliveira, Avelino, Mazzetto, & Lomonaco, 2020). This effect occurs through the addition of acetyl groups to the C2, C3 (corroborated by the presence of small amounts of 3,4- and 2,4-Man linkages identified in Table 2) and C6 positions of mannose, especially favouring the C6 due to a more available position for chemical acetylation (Campestrini, Silveira, Duarte, Koop, & Noseda, 2013; Simões et al., 2010). If one accounts for these factors, the DB calculation can be adjusted assuming that the 4,6-Man available as side chains are only the ones that correspondent to the T-Gal units, namely DB* = (4-Man+T-Gal+T-Man)/T-Gal (Table 2).

Glycosidic linkage analyses were carried out on 3 representative samples, obtained after microwave treatments: 0.1/135/4 is representative of a sample with high viscosity (Table 2, HV), 0.1/165/2 is representative of a condition with low viscosity (Table 2, LV), and 0.3/

Table 2
Glycosidic linkage profile (relative molar ratio, %) of the untreated LBG batch 1 and after microwave (MW) treatments; and of the optimized MW condition of the LBG from batch 2 and corresponding retentate fractions resulting from the ultrafiltration (UF) process carried out with different cut-off membranes. Sugar analysis is also shown in brackets for each sugar residue for comparison purposes.

		LBG batch 1				LBG batch 2						
		Untreated	0.1/135/4 (HV)	0.3/150/3 (CP)	0.1/165/2 (LV)	Untreated	0.3/150/3 (CP)	UF R300	UF R100	UF R50	UF R30	UF R10
UF η (%)		**–**	**–**	**–**	**–**	**–**	**–**	16.7	4.8	3.7	1.6	2.5
Sugar	**Linkage**											
Ara	T-Ara*f*	0.2	0.4	0.2	0.2	–	0.03	0.04	–	0.03	0.01	–
	T-Ara*p*	0.2	0.2	–	0.1	–	–	–	–	–	–	–
	5-Ara*f*	0.6	1.6	0.6	0.5	1.3	0.08	0.27	0.2	0.07	0.05	–
	Total Ara	**1.0 (0.8)**	**2.1 (1.9)**	**0.8 (1.6)**	**0.8 (1.1)**	**1.3 (1.2)**	**0.1 (0.6)**	**0.3(0.5)**	**0.2 (0.4)**	**0.1 (0.1)**	**0.1 (0.8)**	**−(0.2)**
Man	T-Man	1.0	1.0	3.0	2.5	1.7	2.8	2.1	3.1	2.9	2.6	2.5
	4-Man	36.3	37.8	43.3	41.4	47.7	51.1	47.8	49.9	48.5	50.3	52.2
	2,4-Man	0.2	0.2	0.2	0.3	–	0.3	–	–	0.3	0.3	0.3
	3,4-Man	–	–	–	0.2	–	0.2	0.2	–	0.2	0.3	0.2
	4,6-Man	35.3	31.8	26.7	29.8	17.0	25.2	29.0	27.2	26.6	26.3	27.0
	Total Man	**72.8 (69.8)**	**70.8 (64.5)**	**73.1 (67.9)**	**74.2 (70.5)**	**69.3 (73.9)**	**79.6 (79.3)**	**78.8 (74.6)**	**80.0 (77.2)**	**78.5 (76.5)**	**79.8 (75.4)**	**82.2 (79.2)**
Gal	T-Gal	25.4	24.3	25.0	24.4	14.8	17.5	18.0	16.6	19.0	17.7	15.8
	Total Gal	**25.5 (28.5)**	**24.3 (30.4)**	**25.0 (28.3)**	**24.4 (26.9)**	**14.8 (22.4)**	**17.5 (19.8)**	**18.0 (24.3)**	**16.6 (22.1)**	**19.0 (22.3)**	**17.7 (23.8)**	**15.8 (20.1)**
Glc	T-Glc	0.1	1.8	0.7	0.2	–	–	–	–	–	–	–
	4-Glc	0.7	1.0	0.5	0.5	5.6	0.9	2.1	1.7	0.7	0.9	1.3
	Total Glc	**0.8 (1.0)**	**2.8 (3.3)**	**1.2 (2.2)**	**0.7 (1.4)**	**5.6 (2.4)**	**0.9 (0.9)**	**2.1 (1.1)**	**1.7 (0.7)**	**0.7 (0.1)**	**0.9 (0.8)**	**1.3 (0.7)**
M/G ratio		**2.8 (2.4)**	**2.1**	**2.4**	**2.6**	**4.7 (3.3)**	**4.4**	**4.2**	**4.6**	**4.0**	**4.3**	**5.0**
DB*		**2.5**	**2.6**	**2.9**	**2.8**	**4.5**	**4.1**	**3.8**	**4.2**	**3.8**	**4.0**	**4.5**

The M/G ratio was estimated by dividing the total Man residues by the total of Gal residues obtained by sugar analysis (values between brackets). Abbreviations: Ara, arabinose; CP, central point; DB*, degree of branching (estimated as DB* = (4-Man+T-Gal+T-Man)/T-Gal); Man, mannose; Gal, galactose; Glc, glucose, '–', not detected. The series of sugars was considered the same as that occurring in nature: Ara, L-series; hexoses, D-series. All hexoses showed to be present in pyranose form, and Ara occurred both in the furanose and pyranose forms. HV – High viscosity sample; CP – central point design; LV – Low viscosity sample.

150/3 is the central point (Supplementary Table S1; Table 2, CP). The central point revealed molecular weight and viscosity properties (Fig. 1) that were attributed to the low-viscosity samples. As observed in Table 2, minor differences were detected in the sugar composition among the untreated and MW-treated samples, showing a variation between 2.1–2.8 and 2.5–2.9 for M/G and DB respectively, suggesting that under the conditions tested, the MW treatment resulted in depolymerization rather than debranching of the GM. This observation is corroborated by the carbohydrate microarray analysis of these fractions with the anti-galactomannan mAb CCRC-M70 (Fig. 1), which showed a strong binding to batch 1, with a lower M/G ratio, significantly decreasing the avidity after the MW treatment.

The glycosidic linkage profile determined for the retentate fractions resulting from the ultrafiltration (Table 2) corroborated the previous predominant linkages, with 4-linked Man (48 %–52 %), 4,6-linked Man (25 %–29 %), and terminally linked Gal (16 %–19 %). The DB and M/G ratio from both crude and treated samples showed slight alterations, with values ranging from 3.8–4.5 and 4.1–5.0 respectively. It is possible to assess from these results how the partial hydrolysis promoted a viscosity reduction with almost no impact on the branching degree of the polysaccharide. The last permeate fraction (<10 kDa) contains polymeric, oligomeric but also high amounts of monomeric compounds that do not contribute to a polymeric content, and therefore was not considered for the glycosidic analysis. In the following sections, the application of the GMs studied will be assessed as insulin carriers to be delivered by the pulmonary path.

3.3. Galactomannan characteristics for an efficient pulmonary delivery

To determine the influence of Mw on particle characteristics, the different fractions were spray-dried in the presence of insulin, aiming to obtain a shape and size distribution that would better fit the dimensions for efficient pulmonary delivery.

3.3.1. Influence of the molecular weight on microparticle morphology and dimensions

After the spray drying process, the resulting particles were presented as a white powder (<6 % humidity), with a recovery yield of 65 ± 4 %. Losses of material are associated with depositions on the equipment walls, which can compromise the free-flow of the samples through the

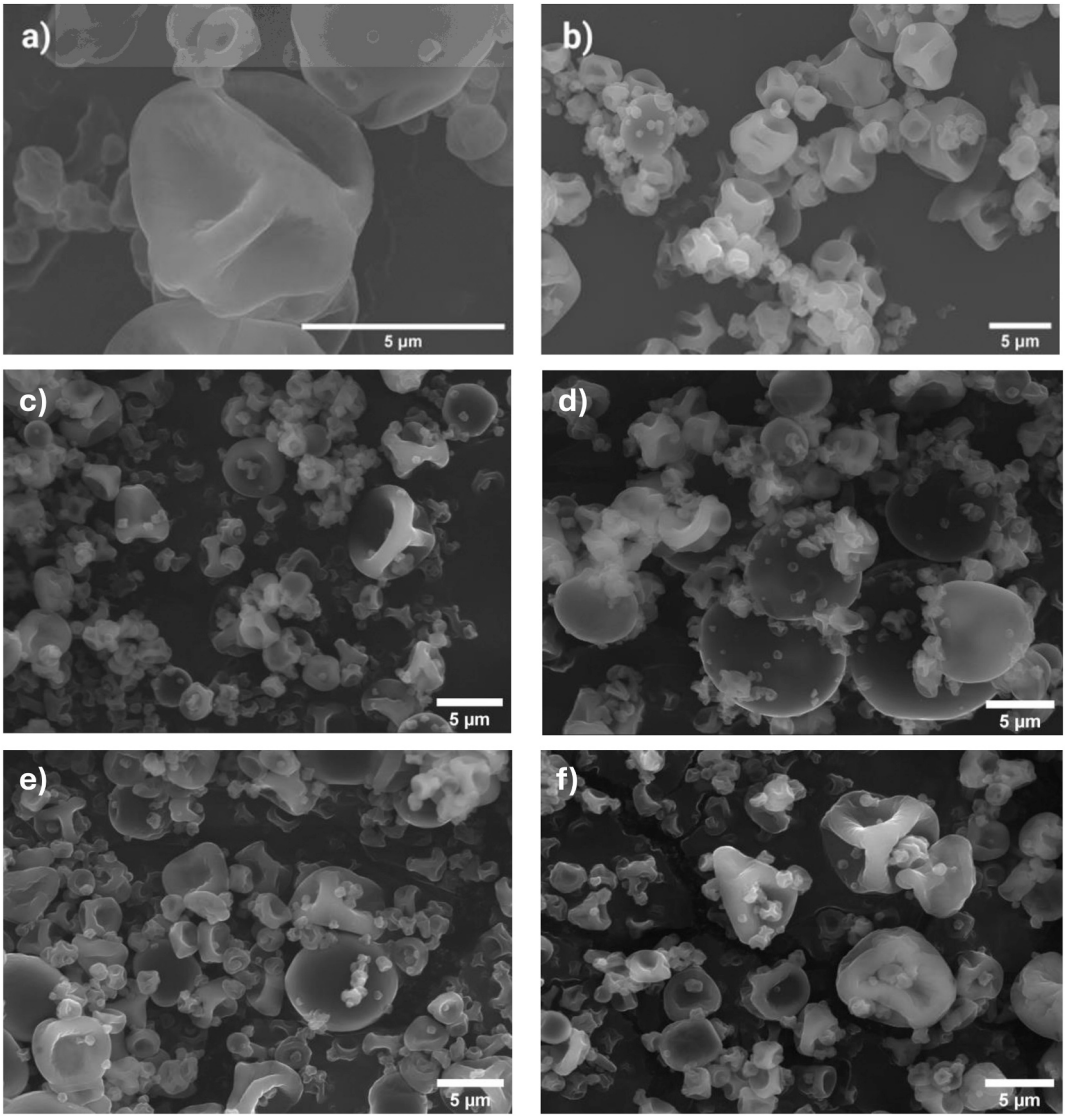

Fig. 3. SEM images (obtained using 15 kV voltage) for LBG Mp after microwave treatment without insulin addition with a) 10 k× ampliation; and b) 3.0 k× ampliation, respectively. SEM images obtained (obtained using 25 kV voltage and 3.0 k× ampliation) after insulin addition (1:10 insulin: total mass, w/w) atomize under growing mass concentrations, respectively corresponded to a viscosity of c) 0.02 Pa·s, d) 0.04 Pa·s, e) 0.09 Pa·s, and f) 0.20 Pa·s (viscosity and concentration correlation can be found in Supplementary Fig. S3).

spray-dryer nozzle, affecting the final yield (Sobulska & Zbicinski, 2021). Nevertheless, the values are within the literature findings when using similar laboratory spray-dryers (Alves et al., 2016; de Almeida et al., 2015). Fig. 3 shows SEM images of the microparticles obtained by spray-drying using the LBG sample after microwave treatment (without the addition of insulin) (Fig. 3a and b). In terms of size, all samples are within a micron scale and can be further considered microparticles (Mp). The formulated Mp presents an irregular raisin-like surface for the most diluted concentrations (Fig. 3a and b). With the addition of insulin, maintaining a constant ratio of 1:10 (insulin: total mass, *w*/w) under diluted conditions (~0.02 Pa·s), the microparticle's irregular raisin-like shape and size (1–5 μm) did not change (Fig. 3c). However, as the mass concentration increased to 0.04 Pa·s (Fig. 3d), 0.09 Pa·s (Fig. 3e), and 0.20 Pa·s (Fig. 3f), the shape changed to a smooth egg shape. The parameter that can influence the particle's morphology is the wetness of the droplet during the spray-drying, as the coalescence of wet droplets can lead to the formation of larger and spherical structures (Eijkelboom et al., 2023). The morphology observed for LBG galactomannans containing insulin was also observed for insulin carriers assembled with galactomannans originating from coffee (Valente et al., 2023). Similar morphology was shown when using LBG batch 1 or 2, showing that the M/G was not a distinction parameter for this effect.

The SEM images show microparticles obtained using the retentate fractions (after microwave treatment and ultrafiltration fractionation) combined with insulin (1:10 insulin: total mass, w/w), respectively using the retentates of 300 kDa (MpR300, Fig. 4a), 100–300 kDa (MpR100, Fig. 4b), 50–100 kDa (MpR50, Fig. 4c), and the retentate of 10–30 kDa (MpR10, Fig. 4d). The formulated Mp using retentates also presents irregular raisin-like surfaces, especially for the samples with higher molecular weight fractions (Fig. 3c–e). On the other hand, the sample containing the lowest molecular weight (Fig. 3f, MpR10, with 10–30 kDa) showed a higher amount of egg-like shape forms with a smoother surface and bigger size.

These results show how particle size is affected by the composition of the samples. In general, the size of microparticles made by low-molecular-weight GMs was larger than that of high-molecular-weight GMs. This effect may also be the result of higher hygroscopicity associated with the lower-size polymers, especially when associated with a higher density of hydrophobic interactions that can contribute to the aggregation of microparticles (Ramos-Hernández, Lagarón, Calderón-Santoyo, Prieto, & Ragazzo-Sánchez, 2021). During the spray-drying due to their higher hygroscopic nature, collisions between semi-dried droplets can increase the possible hypothesis for agglomeration.

Mp distribution for the samples presented in Fig. 4 can be found in supplementary Fig. S4 (Supplementary material). Although the deposition of microparticles in the lower airways is highly dependent on size (1–5 μm), the morphology of these carriers is also an important parameter for pulmonary delivery. The best aerodynamic properties for pulmonary delivery have been associated with non-spherical and rougher surfaced particles. These characteristics allow a low contact area, less formation of aggregates, as well as higher movement resistance in the lung and therefore allow for better flowability (Frota et al., 2018; Mortensen, Durham, & Hickey, 2014). The morphology of the obtained microparticles (Fig. 4) is thus indicative of adequate flowability, showing how the galactomannan particles can be favorable carriers for pulmonary delivery. The cumulative batch of the Mp volume (Fig. 5) shows that all conditions fit the lower dimension requirement, meaning that the Mp is always bigger than 1 μm. Samples with >300 kDa and 100–300 kDa led to the formation of the smaller Mp, achieving almost 40 % within the desired range (1–5 μm) for pulmonary administration (Valente et al., 2022). However, the initial content as starting raw material was significantly higher for the MpR300 sample (16.7 versus 4.8 % recovery, Table 2).

This effect has already been observed in literature applied to nanoparticles, where the use of larger polymers induced the formation of nanoparticles with smaller dimensions (Shimmin, Schoch, & Braun, 2004). Accordingly, the MpR10 sample demonstrated microparticles with the highest dimensions, with <10 % within 1–5 μm, and where 4 % even surpassed 10 μm.

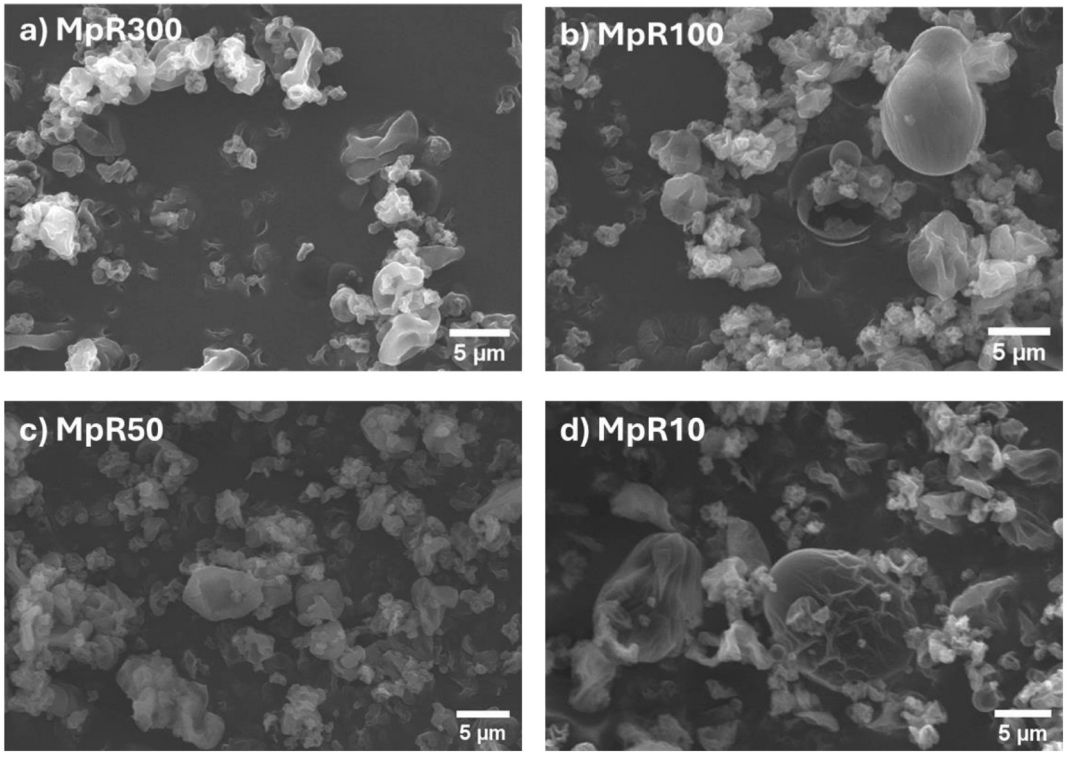

Fig. 4. SEM images obtained (obtained using 25 kV voltage and 1.5 k× ampliation) after insulin addition (1:10 insulin: total mass, w/w) for LBG retentate fractions (obtained after microwave treatment and ultrafiltration fractionation) atomized using: a) the retentate fractions of MpR300; b) MpR100; c) MpR50 and d) MpR10.

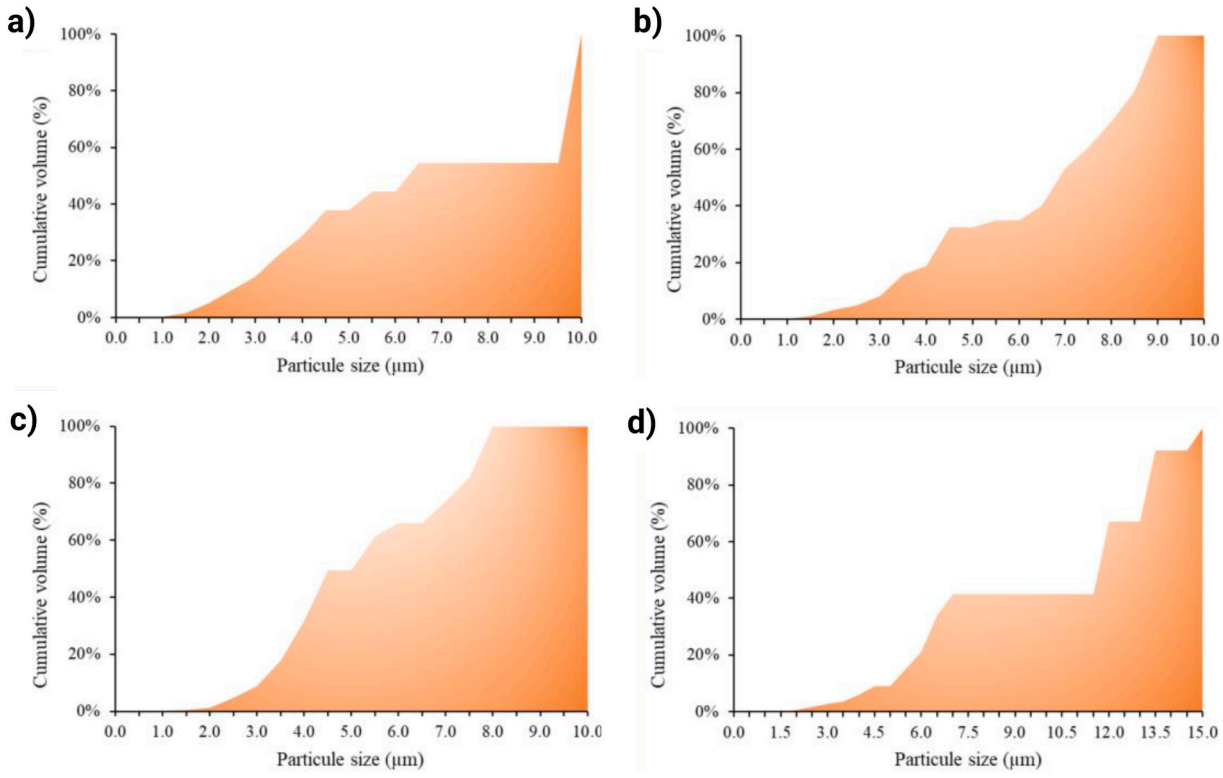

Fig. 5. Microparticles (Mp) cumulative volume (%) according to the particle size for: a) MpR300; b) MpR100; c) MpR50; d) MpR10.

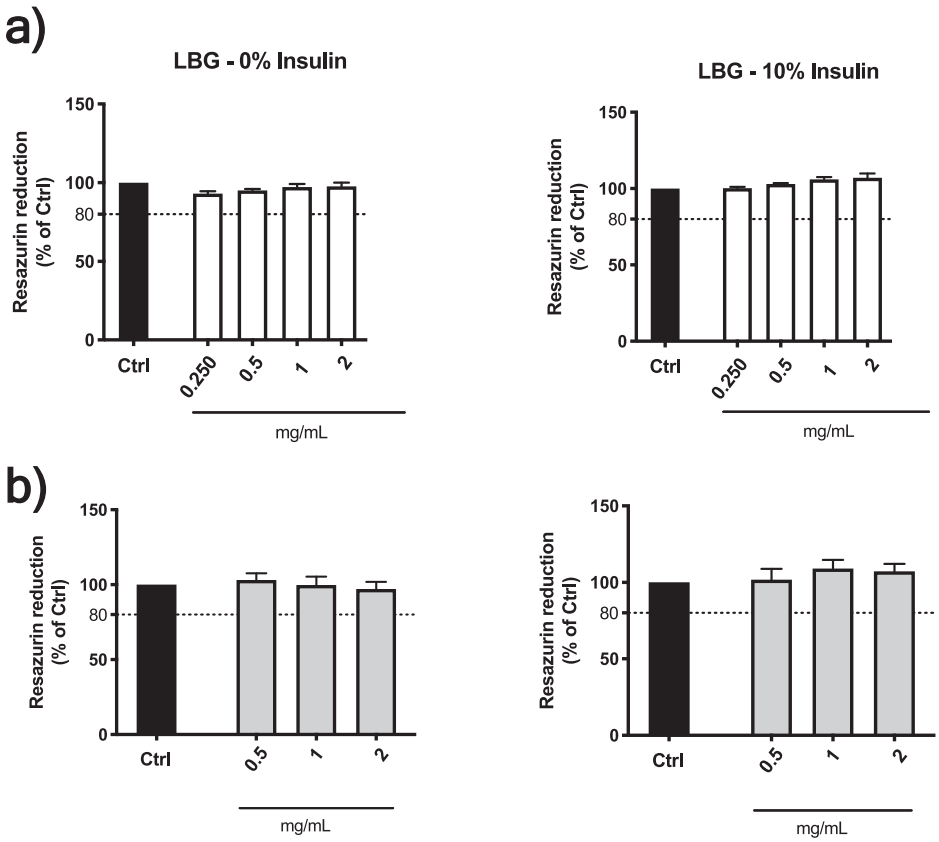

Fig. 6. Effect of Mp on cellular viability in the presence of Mp containing LBG alone (left) or Mp containing LBG and insulin (10 %, *w*/w) (right). a) Human alveolar epithelial cells (A549 cell line) were exposed to Mp for 24 h. b) Macrophages (Raw 264.7 cell line) were exposed to MPs for 24 h. Data correspond to the means ± SEM of at least three independent experiments performed in duplicate and are represented as % of untreated cells (Ctrl). Statistical analysis: one-way ANOVA with Dunnett's multiple comparison test, with no significant differences reported when compared to Ctrl.

3.3.2. Cytotoxicity

Cytotoxicity assays were conducted in the respiratory cell line A549, representative of type II pneumocytes, using polysaccharide based Mp ranging from 0.125 mg/mL to 2 mg/mL. As depicted in Fig. 6a, in A549 cells, LBG alone or containing 10 % insulin showed no cytotoxicity in all the concentrations tested. Considering these results, cell viability was also evaluated on macrophages (Raw 264.7 cell line), cells that also populate the respiratory tract, using 2 mg/mL and below. As shown in Fig. 6b, all Mp proved to be non-cytotoxic.

3.3.3. Insulin quantification and release kinetics

All insulin-loaded Mp were analyzed for their insulin content and delivery capacity. HPLC chromatography revealed one peak around 8.2 min after injection, which corresponds to insulin (Fig. S5a, Supplementary material). A second peak was also observed after the insulin peak (Fig. S5b, Supplementary material), being more evident on the aliquots taken at the end of the delivery process. This small and broad peak probably corresponds to deamidated insulin. Deamidation of insulin may occur in a non-enzymatic way, corresponding to the removal of the amide group on asparagine or glutamine residues (Andrasi et al., 2020). The cause of deamidation can be associated with various parameters such as temperature, agitation, pH, or even during storage. The acidic pH (~4) medium that is used to assemble the Mp can be enough to promote this slight deamidation (Andrasi et al., 2020). Nevertheless, this peak is <3 %, and can therefore be considered neglectable to an insulin activity reduction. In total, and despite the initial 10 % insulin used in all cases (1:10 insulin: total mass, w/w), after 1 h under strong agitation, the HPLC results showed an average recovery of 7.4 ± 0.8 % of insulin. This value is then converted to 100 % of the total available insulin.

Insulin release kinetics is a parameter of high importance as it may dictate hypo- and hyperglycemia effects. Galactomannans, due to their swelling ability can be useful for Mp preparation as the pore sizes in the Mp can change due to the alteration of the polysaccharide conformation when it expands. This characteristic is a good advantage for the control of the retention and release of insulin: first, the small pores would prevent insulin release, but as the swelling occurs it could easily lead to insulin loss by simple diffusion (Quesada-Pérez, Maroto-Centeno, Forcada, & Hidalgo-Alvarez, 2011). To evaluate the insulin release kinetics, delivery assays were performed using an orbital incubator, with temperature (37 °C) and agitation (100 rpm) conditions that would better simulate the lung's environment. Fig. 7 represents the delivery process of the samples over 60 min, with all insulin content being delivered at this time. Although the results for the Mp from different-sized polymers were similar, the behaviour during the delivery showed some differences. It can be observed that the release of insulin reaches approximately 100 % on all available Mp. The time required to achieve such value varied depending on the fraction used for the Mp preparation. The microparticles containing polymers with >300 kDa (MpR300, Fig. 7a), 100–300 kDa (MpR100, Fig. 7b), and 50–100 kDa (MpR100, Fig. 7c) require approximately 40 min to achieve the maximum release, while the Mp of MpR10 (containing polymers with 10–30 kDa) showed an almost complete delivery after only 20 min (Fig. 7d). The results were confirmed in the 2 replicated experiments. After the spray-drying process, the polysaccharide becomes more compact, making it harder for water molecules to dissolve the material. Because galactomannans with higher dimensions show higher viscosity, the water will penetrate the microparticle at a slower rate (Vendruscolo, Andreazza, Ganter, Ferrero, & Bresolin, 2005), consequentially leading to a more gradual release from the carrier. The higher hygroscopicity for low Mw GMs, which has shown a relationship with the particle morphology and dimensions, can also affect the insulin release kinetics. Although smaller Mps can have a

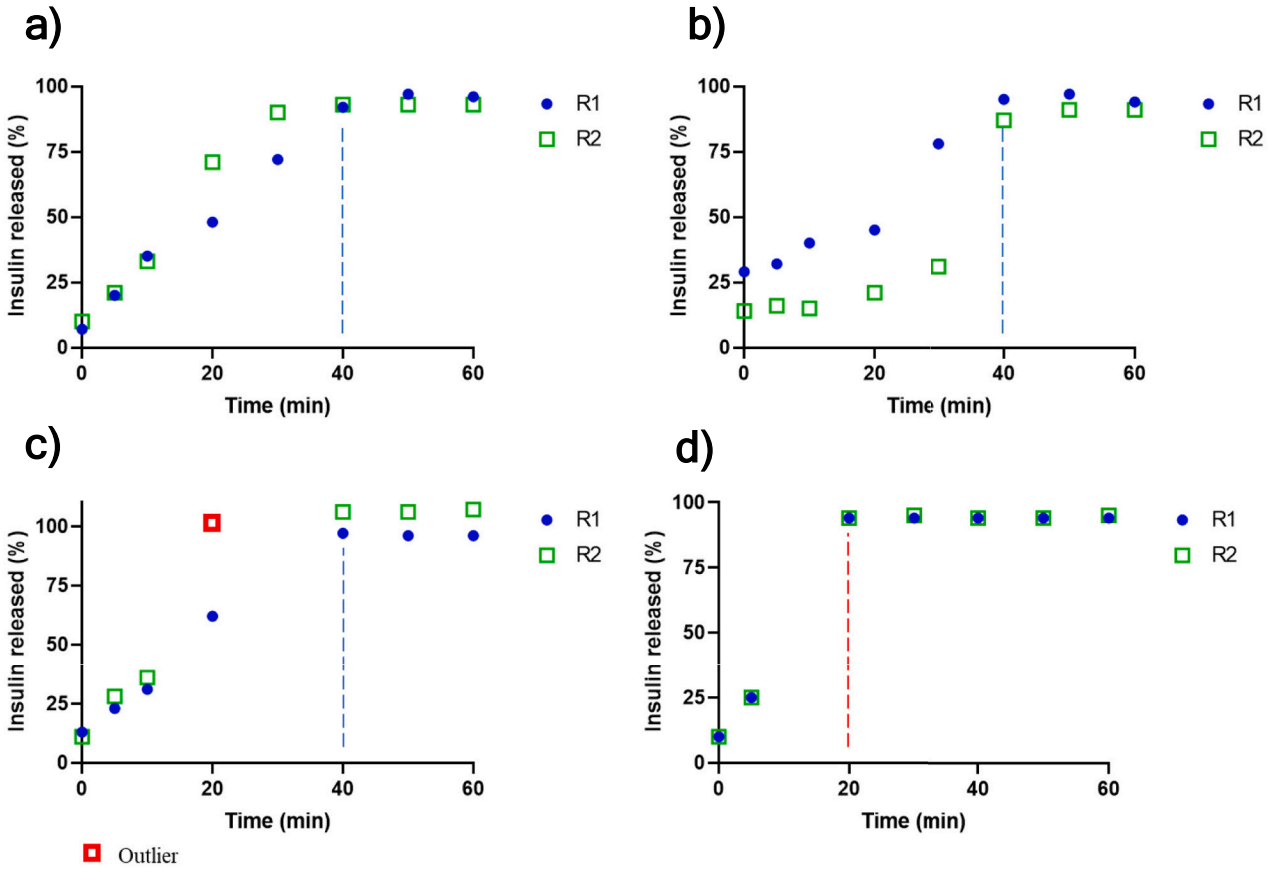

Fig. 7. Microparticle insulin release kinetics throughout 1 h obtained at HPLC for: a) MpR300; b) MpR100; c) MpR50; d) MpR10.

faster diffusion due to an increased surface area-to-volume ratio, the higher hygroscopicity of the smaller Mps, contributing to agglomeration during the spray-drying process, results also in an increased porosity (Eijkelboom et al., 2023). Here, the more porous structures will increase the speed at which the solution is diffused into the interior, hence leading to a faster insulin release.

These results also showed that the polymer size used to assemble Mp will not only influence the particle size (see Fig. 4) but also the delivery behaviour of encapsulated compounds. This conclusion is corroborated by other experiments, for example, studies where PLGA microparticle size and drug kinetics were compared and found how the increased particle size leads to faster degradation of the system, and diffusion of the encapsulated agent (Chen, Palazzo, Hennink, & Kok, 2017; Siepmann, Faisant, Akiki, Richard, & Benoit, 2004). With the exception for the MpR100 (Fig. 7b) that showed a delayed biphasic behaviour, the release behaviour from different Mp (some faster than others) showed the ideal monophasic linear release kinetics (Fig. 7a, c, and d) in vitro (Yoo & Won, 2020). This type of release is desired for drugs with a broader window of therapeutic effect, allowing a constant concentration of the drug in circulation to promote the desired effect, while limiting adverse effects such as potential toxicity (Laracuente, Yu, & McHugh, 2020). The results obtained from this work show the potential to assemble Mp for a faster or slower insulin administration, adapting to each situation.

4. Conclusion

In this work, locust bean gum (LBG) was used as a source of galactomannan (GM), a polysaccharide with the potential to be used for microparticle preparation. Due to GM's high viscosity, suitable conditions of microwave partial acid hydrolysis were tested to depolymerize the polysaccharide, and consequentially reduce its viscosity. A temperature of 150 °C and an acetic acid concentration of 0.3 M were determined as suitable conditions, allowing a viscosity reduction to <0.005 Pa·s. The results showed that the MW treatment resulted in heterogenous depolymerization, with most of the material being recovered as >300 kDa (17 %) and <10 kDa (30 %). The analysis of the different glycosidic linkages and branching degree (DB) showed a small variation between the different fractions: with 4-Man (48–52 %), 4,6-Man (17–29 %), and T-Gal (16–19 %) as major linkages and a DB that varied within 3.8 and 4.5, within the sequential fractions of decreasing molecular weight. These results suggest that the MW treatment allowed depolymerization of the GM without revealing a major impact on the debranching of the polysaccharide. Protein recognition using carbohydrate microarrays pointed to structural differences when using GMs from different batches and after being processed. As both galactomannan batches were from Sigma Aldrich (G0753 - Locust bean gum from *Ceratonia siliqua* seeds), this highlights the need for the chemical characterization of commercial samples for a better interpretation of their properties.

Microparticle assembly, by spray-drying the different fractions with insulin, led to a white powder with an average yield of 65 ± 4 %. Morphological analysis revealed raisin-like structures. Fractions of higher molecular weight led to microparticles of 1–5 μm, while the fraction of low molecular weight led to microparticles with 92 % in a 5–15 μm geometric range. Results showed that particle size could be controlled by changing the concentration and/or Mw of the GM used for particle preparation. The microparticles showed 7.4 % content of insulin loaded into the powder, and the ability for a linear, controlled, and total delivery of its content. The delivery rate was also dependent on polymer Mw: a faster delivery was observed for Mp prepared using lower molecular weight material (20 min) when compared with Mp prepared with GM of dimensions superior to 50 kDa, which required approximately 40 min for total insulin delivery. Nevertheless, in all cases, insulin was delivered in 60 min time-length, an interesting result for developing post-prandial insulin-delivering systems. Therefore, a combination of MW, ultrafiltration, and spray-drying techniques showed potential for microparticle preparation for safe pulmonary delivery of insulin, where the speed of release can be controlled by the galactomannan dimensions.

CRediT authorship contribution statement

Miguel F. Galrinho: Writing – original draft, Investigation, Formal analysis. **Lisete M. Silva:** Writing – review & editing, Writing – original draft, Validation, Investigation, Formal analysis. **Guido R. Lopes:** Writing – review & editing, Data curation. **Bernardo A.C. Ferreira:** Writing – review & editing, Formal analysis. **Sara A. Valente:** Writing – review & editing, Validation, Formal analysis. **Isabel Ferreira:** Writing – review & editing, Formal analysis. **Benedita A. Pinheiro:** Writing – review & editing, Formal analysis. **Angelina S. Palma:** Writing – review & editing, Methodology. **Dmitry V. Evtuguin:** Writing – review & editing, Data curation. **José A. Lopes da Silva:** Writing – review & editing, Data curation. **Margarida Almeida:** Writing – review & editing, Data curation. **Paula Ferreira:** Writing – review & editing, Data curation. **Maria T. Cruz:** Writing – review & editing, Data curation. **Manuel A. Coimbra:** Writing – review & editing, Supervision, Resources, Methodology, Data curation, Conceptualization. **Cláudia P. Passos:** Writing – review & editing, Visualization, Validation, Supervision, Resources, Project administration, Methodology, Investigation, Funding acquisition, Data curation, Conceptualization.

Declaration of competing interest

The authors declare that there is no potential conflict of interest.

Data availability

Data are available upon request.

Acknowledgments

The authors thank Fundação para a Ciência e Tecnologia (FCT) co-financed by Programa Operacional Competitividade e Internacionalização, Portugal 2020 and União Europeia by the FEDER (FCT - Compete2020 - Portugal 2020 – FEDER/EU) N° POCI-01-0145-FEDER-029560, the project "PulManCar". Thanks are also due to the University of Aveiro and FCT for the financial support for the LAQV-REQUIMTE (UIDB/50006/2020), and CICECO-Aveiro Institute of Materials, UIDB/50011/2020 (DOI 10.54499/UIDB/50011/2020), UIDP/50011/2020 (DOI 10.54499/UIDP/50011/2020) & LA/P/0006/2020 (DOI 10.54499/LA/P/0006/2020) and CEF, UIDB/00239/2020, both Centres financed by national funds through the FCT/MCTES (PIDDAC). Lisete M. Silva contract, Sara Valente, and Isabel Ferreira MSc. grants were supported by project "PulManCar". Sara Valente and Cláudia Passos thank FCT for the individual grant (DFA/BD/5430/2020) and for funding through the Individual Call to Scientific Employment Stimulus (https://doi.org/10.54499/CEECIND/00813/2017/CP1459/CT0053), respectively.

Appendix A. Supplementary data

Supplementary data to this article can be found online at https://doi.org/10.1016/j.carbpol.2024.122268.

References

Alves, A. D., Cavaco, J. S., Guerreiro, F., Lourenço, J. P., Rosa Da Costa, A. M., & Grenha, A. (2016). Inhalable antitubercular therapy mediated by locust bean gum microparticles. *Molecules, 21*(6).

Amidi, M., Pellikaan, H. C., de Boer, A. H., Crommelin, D. J. A., Hennink, W. E., & Jiskoot, W. (2008). Preparation and physicochemical characterization of supercritically dried insulin-loaded microparticles for pulmonary delivery. *European Journal of Pharmaceutics and Biopharmaceutics, 68*(2), 191–200.

Andrasi, M., Pajaziti, B., Sipos, B., Nagy, C., Hamidli, N., & Gaspar, A. (2020). Determination of deamidated isoforms of human insulin using capillary electrophoresis. *J. Chromatogr. A*, 1626.
Arpagaus, C., & Meuri, M. (2010). Laboratory scale spray drying of inhalable particles: a review. *Respiratory Drug Deliv.*, 469–473.
Avachat, A. M., Dash, R. R., & Shrotriya, S. N. (2011). Recent investigations of plant based natural gums, mucilages and resins in novel drug delivery systems. *Indian Journal Of Pharmaceutical Education And Research, 45*(1), 86–99.
Brito-Oliveira, T. C., Cavini, A. C. M., Ferreira, L. S., Moraes, I. C. F., & Pinho, S. C. (2020). Microstructural and rheological characterization of NaCl-induced gels of soy protein isolate and the effects of incorporating different galactomannans. *Food Structure, 26*, 100158.
Campestrini, L. H., Silveira, J. L. M., Duarte, M. E. R., Koop, H. S., & Noseda, M. D. (2013). NMR and rheological study of Aloe barbadensis partially acetylated glucomannan. *Carbohydrate Polymers, 94*(1), 511–519.
Cardoso, S. M., Coimbra, M. A., & Lopes da Silva, J. A. (2003). Temperature dependence of the formation and melting of pectin–Ca2+ networks: A rheological study. *Food Hydrocolloids, 17*(6), 801–807.
Cavaiola, T. S., & Edelman, S. (2014). Inhaled insulin: A breath of fresh air? A review of inhaled insulin. *Clinical Therapeutics, 36*(8), 1275–1289.
Cerqueira, M. A., Pinheiro, A. C., Souza, B. W. S., Lima, Á. M. P., Ribeiro, C., Miranda, C., … Vicente, A. A. (2009). Extraction, purification and characterization of galactomannans from non-traditional sources. *Carbohydrate Polymers, 75*(3), 408–414.
Chaires-Martínez, L., Salazar-Montoya, J. A., & Ramos-Ramírez, E. G. (2008). Physicochemical and functional characterization of the galactomannan obtained from mesquite seeds (Prosopis pallida). *European Food Research and Technology, 227*(6), 1669–1676.
Chen, W., Palazzo, A., Hennink, W. E., & Kok, R. J. (2017). Effect of particle size on drug loading and release kinetics of gefitinib-loaded PLGA microspheres. *Molecular Pharmaceutics, 14*(2), 459–467.
Ciucanu, I., & Kerek, F. (1984). A simple and rapid method for the permethylation of carbohydrates. *Carbohydrate Research, 131*(2), 209–217.
Coimbra, M. A., Delgadillo, I., Waldron, K. W., & Selvendran, R. R. (1996). Isolation and analysis of cell wall polymers from olive pulp. In H. F. Linskens, & J. F. Jackson (Eds.), *Plant Cell Wall Analysis* (pp. 19–44). Berlin, Heidelberg: Springer Berlin Heidelberg.
de Almeida, R. R., Magalhães, H. S., de Souza, J. R. R., Trevisan, M. T. S., Vieira, I. G. P., Feitosa, J. P. A., … Ricardo, N. M. P. S. (2015). Exploring the potential of Dimorphandra gardneriana galactomannans as drug delivery systems. *Industrial Crops and Products, 69*, 284–289.
de Oliveira, D. R., Avelino, F., Mazzetto, S. E., & Lomonaco, D. (2020). Microwave-assisted selective acetylation of Kraft lignin: Acetic acid as a sustainable reactant for lignin valorization. *International Journal of Biological Macromolecules, 164*, 1536–1544.
Dionísio, M., & Grenha, A. (2012). Locust bean gum: Exploring its potential for biopharmaceutical applications. *Journal of Pharmacy & Bioallied Sciences, 4*(3), 175–185.
Eijkelboom, N. M., van Boven, A. P., Siemons, I., Wilms, P. F. C., Boom, R. M., Kohlus, R., & Schutyser, M. A. I. (2023). Particle structure development during spray drying from a single droplet to pilot-scale perspective. *Journal of Food Engineering, 337*, 111222.
Frota, H. B. M., Menezes, J. E. S. A., Siqueira, S. M. C., Ricardo, N. M. P., Araújo, T. G., Souza, C. A. G., … Dos Santos, H. S. (2018). Preparation, physicochemical characterization and controlled release of galactomannan microparticles containing allantoin. *Química Nova, 41*(5), 544–549.
Gowda, D. V., Gupta, N. V., Khan, M. S., & Singh, M. N. (2011). Development and evaluation of modified locust bean microparticles for controlled drug delivery. *Latin American Journal of Pharmacy, 30*(3), 519–526.
Harris, P. J., Henry, R. J., Blakeney, A. B., & Stone, B. A. (1984). An improved procedure for the methylation analysis of oligosaccharides and polysaccharides. *Carbohydrate Research, 127*(1), 59–73.
Hellebois, T., Soukoulis, C., Xu, X., Hausman, J.-F., Shaplov, A., Taoukis, P. S., & Gaiani, C. (2021). Structure conformational and rheological characterisation of alfalfa seed (Medicago sativa L.) galactomannan. *Carbohydrate Polymers, 256*, Article 117394.
Kök, M. S. (2007). A comparative study on the compositions of crude and refined locust bean gum: In relation to rheological properties. *Carbohydrate Polymers, 70*(1), 68–76.
Kontogiorgos, V. (2019). Galactomannans (guar, locust bean, fenugreek, tara). In L. Melton, F. Shahidi, & P. Varelis (Eds.), *Encyclopedia of food chemistry* (pp. 109–113). Oxford: Academic Press.
Laracuente, M. L., Yu, M. H., & McHugh, K. J. (2020). Zero-order drug delivery: State of the art and future prospects. *Journal of Controlled Release, 327*, 834–856.
Lazaridou, A., Biliaderis, C. G., & Izydorczyk, M. S. (2001). Structural characteristics and rheological properties of locust bean galactomannans: A comparison of samples from different carob tree populations. *Journal of the Science of Food and Agriculture, 81*(1), 68–75.
Lee, N., Amy, G., Croué, J.-P., & Buisson, H. (2004). Identification and understanding of fouling in low-pressure membrane (MF/UF) filtration by natural organic matter (NOM). *Water Research, 38*(20), 4511–4523.
Liu, Y., Childs, R. A., Palma, A. S., Campanero-Rhodes, M. A., Stoll, M. S., Chai, W., & Feizi, T. (2012). Neoglycolipid-based oligosaccharide microarray system: Preparation of NGLs and their noncovalent immobilization on nitrocellulose-coated glass slides for microarray analyses. *Methods in Molecular Biology, 808*, 117–136.
Liu, Y., McBride, R., Stoll, M., Palma, A. S., Silva, L., Agravat, S., … Smith, D. F. (2016). The minimum information required for a glycomics experiment (MIRAGE) project: Improving the standards for reporting glycan microarray-based data. *Glycobiology, 27*(4), 280–284.
McCleary, B. V., Amado, R., Waibel, R., & Neukom, H. (1981). Effect of galactose content on the solution and interaction properties of guar and carob galactomannans. *Carbohydrate Research, 92*(2), 269–285.
Mccleary, B. V., Clark, A. H., Dea, I. C. M., & Rees, D. A. (1985). The fine-structures of carob and guar galactomannans. *Carbohydrate Research, 139*(Jun), 237–260.
Morales, F. J., & van Boekel, M. A. J. S. (1998). A study on advanced Maillard reaction in heated casein/sugar solutions: Colour formation. *International Dairy Journal, 8*(10), 907–915.
Mortensen, N. P., Durham, P., & Hickey, A. J. (2014). The role of particle physico-chemical properties in pulmonary drug delivery for tuberculosis therapy. *Journal of Microencapsulation, 31*(8), 785–795.
Palma, A. S., Liu, Y., Zhang, H., Zhang, Y., McCleary, B. V., Yu, G., … Chai, W. (2015). Unravelling glucan recognition systems by glycome microarrays using the designer approach and mass spectrometry. *Molecular and Cellular Proteomics, 14*(4), 974–988.
Passos, C. P., Cepeda, M. R., Ferreira, S. S., Nunes, F. M., Evtuguin, D. V., Madureira, P., … Coimbra, M. A. (2014). Influence of molecular weight on in vitro immunostimulatory properties of instant coffee. *Food Chemistry, 161*, 60–66.
Passos, C. P., & Coimbra, M. A. (2013). Microwave superheated water extraction of polysaccharides from spent coffee grounds. *Carbohydrate Polymers, 94*(1), 626–633.
Passos, C. P., Costa, R. M., Ferreira, S. S., Lopes, G. R., Cruz, M. T., & Coimbra, M. A. (2021). Role of coffee caffeine and chlorogenic acids adsorption to polysaccharides with impact on brew immunomodulation effects. *Foods, 10*(2).
Passos, C. P., Moreira, A. S. P., Domingues, M. R. M., Evtuguin, D. V., & Coimbra, M. A. (2014). Sequential microwave superheated water extraction of mannans from spent coffee grounds. *Carbohydrate Polymers, 103*(0), 333–338.
Passos, C. P., Rudnitskaya, A., Neves, J. M. M. G. C., Lopes, G. R., & Coimbra, M. A. (2019). Data on yields, sugars and glycosidic-linkage analyses of coffee arabinogalactan and galactomannan mixtures and optimization of their microwave assisted extraction from spent coffee grounds. *Data in Brief, 24*.
Passos, C. P., Rudnitskaya, A., Neves, J. M. M. G. C., Lopes, G. R., Evtuguin, D. V., & Coimbra, M. A. (2019). Structural features of spent coffee grounds water-soluble polysaccharides: Towards tailor-made microwave assisted extractions. *Carbohydrate Polymers, 214*, 53–61.
Prajapati, V. D., Jani, G. K., Moradiya, N. G., Randeria, N. P., & Nagar, B. J. (2013). Locust bean gum: A versatile biopolymer. *Carbohydrate Polymers, 94*(2), 814–821.
Quesada-Pérez, M., Maroto-Centeno, J. A., Forcada, J., & Hidalgo-Alvarez, R. (2011). Gel swelling theories: The classical formalism and recent approaches. *Soft Matter, 7*(22), 10536–10547.
Ramos-Hernández, J. A., Lagarón, J. M., Calderón-Santoyo, M., Prieto, C., & Ragazzo-Sánchez, J. A. (2021). Enhancing hygroscopic stability of agave fructans capsules obtained by electrospraying. *Journal of Food Science and Technology, 58*(4), 1593–1603.
Reis, S. F., Messias, S., Bastos, R., Martins, V. J., Correia, V. G., Pinheiro, B. A., … Coelho, E. (2023). Structural differences on cell wall polysaccharides of brewer's spent Saccharomyces and microarray binding profiles with immune receptors. *Carbohydrate Polymers, 301*.
Ribeiro, D. O. (2020). *Protein-carbohydrate recognition in the biodegradation of the plant cell wall: Functional and structural studies using carbohydrate microarrays and X-ray crystallography* (PhD Thesis, School of Science and Technology). NOVA University of Lisbon.
Rodrigues, S., Alves, A. D., Cavaco, J. S., Pontes, J. F., Guerreiro, F., Rosa da Costa, A. M., … Grenha, A. (2017). Dual antibiotherapy of tuberculosis mediated by inhalable locust bean gum microparticles. *International Journal of Pharmaceutics, 529*(1), 433–441.
Schneider, C. A., Rasband, W. S., & Eliceiri, K. W. (2012). NIH image to ImageJ: 25 years of image analysis. *Nature Methods, 9*(7), 671–675.
Shimmin, R. G., Schoch, A. B., & Braun, P. V. (2004). Polymer size and concentration effects on the size of gold nanoparticles capped by polymeric thiols. *Langmuir, 20*(13), 5613–5620.
Siepmann, J., Faisant, N., Akiki, J., Richard, J., & Benoit, J. P. (2004). Effect of the size of biodegradable microparticles on drug release: Experiment and theory. *Journal of Controlled Release, 96*(1), 123–134.
Simões, J., Nunes, F. M., Domingues, M. D. M., & Coimbra, M. A. (2010). Structural features of partially acetylated coffee galactomannans presenting immunostimulatory activity. *Carbohydrate Polymers, 79*(2), 397–402.
Simões, J., Nunes, F. M., Domingues, M. R., & Coimbra, M. A. (2011). Demonstration of the presence of acetylation and arabinose branching as structural features of locust bean gum galactomannans. *Carbohydrate Polymers, 86*(4), 1476–1483.
Sobulska, M., & Zbicinski, I. (2021). Advances in spray drying of sugar-rich products. *Drying Technology, 39*(12), 1774–1799.
Srivastava, M., & Kapoor, V. P. (2005). Seed galactomannans: An overview. *Chemistry & Biodiversity, 2*(3), 295–317.
Stone, K. C., Mercer, R. R., Gehr, P., Stockstill, B., & Crapo, J. D. (1992). Allometric relationships of cell numbers and size in the mammalian lung. *American Journal of Respiratory Cell and Molecular Biology, 6*(2), 235–243.
Valente, S. A., Lopes, G. R., Ferreira, I., Galrinho, M. F., Almeida, M., Ferreira, P., … Passos, C. P. (2023). Polysaccharide-based carriers for pulmonary insulin delivery: The potential of coffee as an unconventional source. *Pharmaceutics, 15*(4), 1213.
Valente, S. A., Silva, L. M., Lopes, G. R., Sarmento, B., Coimbra, M. A., & Passos, C. P. (2022). Polysaccharide-based formulations as potential carriers for pulmonary delivery – A review of their properties and fates. *Carbohydrate Polymers, 277*, 118784.
Vendruscolo, C. W., Andreazza, I. F., Ganter, J. L. M. S., Ferrero, C., & Bresolin, T. M. B. (2005). Xanthan and galactomannan (from M. scabrella) matrix tablets for oral

controlled delivery of theophylline. *International Journal of Pharmaceutics, 296*(1–2), 1–11.
Weibel, E. R. (1963). Chapter VIII-Composition and dimensions of alveolo-capillary tissue barrier. In E. R. Weibel (Ed.), *Morphometry of the human lung* (pp. 89–104). Academic Press.
Weibel, E. R. (2017). Lung morphometry: The link between structure and function. *Cell and Tissue Research, 367*(3), 413–426.
Yoo, J., & Won, Y.-Y. (2020). Phenomenology of the initial burst release of drugs from PLGA microparticles. *ACS Biomaterials Science & Engineering, 6*(11), 6053–6062.